C461/024/93

Gas-particle flow through bends

S JAYANTI, BTech, MS, DEA, PhD, G F HEWITT, PhD, CEng, FIMechE, FEng, FRS and M J MOHIDEEN
Department of Chemical Engineering and Chemical Technology, Imperial College of Science, Technology and Medicine, London
M J WANG, Dr Ing and F MAYINGER, Dr Ing
Lehrstuhl A für Thermodynamik, Technische Universität Munchen, Germany

ABSTRACT Gas-particle motion in 90 and 180-deg bends of circular cross-section is studied using a CFD code. The effect of turbulent dispersion on the particle trajectories is taken into account using a stochastic model. Results indicate that the curvature-induced secondary flow in the gas phase can have a significant effect on the particle motion so that small particles may come out of the bend without depositing. The effect of turbulent dispersion is mainly to increase the likelihood of deposition of small particles.

NOMENCLATURE

c_μ, c_1, c_2	constants in turbulence model
C_D	drag coefficient
d_p	particle diameter
$\boldsymbol{F}$	force vector
k	turbulent kinetic energy
r	radial coordinate
R_c	bend radius
R_t	tube radius
Re	Reynolds number
t	time
t_e	eddy lifetime
$\boldsymbol{V}$	velocity vector
β	bend angle
ε	turbulent dissipation rate
θ	polar coordinate
μ	dynamic viscosity
ξ	spatial position
ϱ	density
σ_k	constant in turbulence model

Subscripts

d	deposition
g	gas
p	particle
r	relative
0	mean parameter at bend inlet

1 INTRODUCTION

As a liquid droplet or a solid particle is carried through a bend, there is a tendency for it to move away from the centre of curvature because of the centrifugal acceleration on it. Such a flow situation is of practical importance, and may have either beneficial or deleterious effect. For example, in heat exchangers in the post-dryout region where there is no liquid film on the wall, the deposition of the liquid droplets in a bend will increase the heat transfer coefficient, and reduce the wall temperature [1,2]. Such curvature-induced deposition can also be used to separate liquid droplets in gas flow which is desirable in turbines and some oil-industry applications. A disadvantageous effect, in the form of increased frictional losses, of particle deposition arises in conveying a solid either by gas or liquid. It can also lead to significant erosion locally. It is clear from these examples that a clear understanding of the particle motion in bends is necessary. This can be done by simulating the trajectory of the particle in the gas flow field. However, the flow of gas through bends is quite complicated (see for example, Ref. [3-5]), and it is necessary to resort to computational fluid dynamics (CFD) techniques to make a realistic estimate of the path of the particle. The present paper describes the results from such a study. It is shown that particle motion can be significantly affected by the secondary flow (i.e., flow in a plane perpendicular to axial direction) in the gas phase as a result of which a particle may not deposit even in a 180-deg bend. This and other

aspects of particle motion are discussed below.

2 METHODOLOGY

CFD techniques for single phase flow have been well-established for a number of years and normally take the form of computer "codes" which can be used to solve for the flow field and heat transfer with appropriate grid, boundary conditions and any other engineering information specific to the problem. The numerical simulations described in the present study were carried out using the Harwell-FLOW3D computer program [6] being developed by the UKAEA. In order to calculate the two-phase flow of gas and particles, the "particle source in cell" method is used. In this method, the flow fields of the two phases are not calculated simultaneously but in alternate steps using source (sink) terms for mass, momentum and energy exchange between the phases. Details of these calculations are given below.

2.1 Calculation of the Gas Flow Field

These calculations were performed using the Harwell-FLOW3D computer program (Release 2.4), which uses a finite difference (volume) method on a general non-orthogonal body-fitted grid. In contrast with most fluid flow algorithms, a non-staggered grid is used in the code with velocity components in fixed Cartesian directions. A modified and three-dimensional version of the Rhie and Chow algorithm [7] is used to overcome the problem of checkerboard oscillations usually associated with the use of non-staggered grids. In the present calculations, the SIMPLEC algorithm [8] is used for pressure-velocity decoupling, and the hybrid differencing scheme is used for the convective term. The standard $k-\varepsilon$ turbulence model [9] is used, and the values for the model constants c_μ, c_1, c_2, σ_k, were set to be equal to 0.09, 1.44, 1.92, and 1.0 respectively. The boundary conditions were as follows. Standard wall functions ("log layers") were used near the walls. At the inlet, i.e., one interval upstream, the velocity field in fully developed flow in a straight tube were specified. At the outlet, fully developed flow was assumed. The effect of using longer upstream and downstream lengths for flow development was investigated [2], but was found to have little effect on the flow field in the bend. Computations were run on HP750/PVRX and SUNSPARC2 workstations and on CRAY-XMP/416. Other computational details can be found in Wang [2].

2.2 Calculation of Particle Trajectories

The particle trajectories are calculated by following the particles in a Lagrangian frame of reference through the flow domain. The path of the particle is obtained by integrating, from given initial conditions of size, position and velocity, an ordinary differential equation representing a force balance on the particle:

$$m_p \frac{\mathrm{d}\boldsymbol{V}_p}{\mathrm{d}t} = \boldsymbol{F} \tag{1}$$

and

$$\frac{\mathrm{d}\xi}{\mathrm{d}t} = \boldsymbol{V}_p \tag{2}$$

Here m_p is the mass of the particle, ξ and $\boldsymbol{V}_p$ its position and velocity, respectively, at any instant, and $\boldsymbol{F}$ the sum of external forces acting on it. In the present study, $\boldsymbol{F}$ consists only of the drag force due to the relative motion between the particle and the fluid surrounding it, and is given by

$$\boldsymbol{F} = \boldsymbol{F}_D = \frac{1}{8}\pi d_p \varrho_g C_D \mid \boldsymbol{V}_r \mid \boldsymbol{V}_r \tag{3}$$

Here d_p is the particle diameter, C_D the drag coefficient, ϱ_g the density of the continuous fluid (gas) and $\boldsymbol{V}_r$ the relative velocity equal to $\boldsymbol{V}_g - \boldsymbol{V}_p$. There are several correlations for the drag coefficient in the literature, and the one employed here [10] is as follows:

$$C_D = 24(1 + 0.15 Re_p^{0.687})/Re_p \tag{4}$$

where the particle Reynolds number is defined as $Re_p = \varrho_g \mid \boldsymbol{V}_r \mid d_p/\mu_g$ where μ_g is the dynamic viscosity of the continuous fluid (gas).

The integration of the above equations is performed until the particle either hits the wall or leaves the flow domain. For ease of computation, these calculations are done in the computational space, and are converted finally into the physical space using the coordinate transformation described in Burns & Wilkes [11].

2.3 Particle Trajectories with Turbulent Dispersion

The effect of the continuous phase turbulence on the motion of particles is taken into account through a stochastic model of the type proposed by Hutchinson et al. [12] and Gosman & Ioannides [13]. Here it is assumed that particle motion is governed mainly by interaction with large, energy-containing eddies.

Thus, the particle, in its motion through the flow domain, is assumed to interact with a series of turbulent eddies. In reality, the eddies change in their size and direction during their life time. However, in the model, it is assumed that an eddy does not lose its identity during its lifetime but that it continues to act on the particle with a constant velocity as long as the particle remains in the eddy. The strength of the eddy is equal to the turbulent kinetic energy k and its lifetime t_e is given by

$$t_e = 1.5^{0.5} c_\mu^{0.75} \frac{k}{\epsilon} \qquad (5)$$

in which c_μ is a turbulence model constant and ϵ is the energy dissipation rate. During the time the particle stays in the eddy, the fluid velocity is composed of the local mean fluid velocity and a fluctuating velocity due to the eddy. The interaction ends when either the particle leaves or the eddy suddenly dies. The particle then begins to interact with a new eddy.

Since the model is stochastic, a large number of simulations of particle trajectories is necessary to accurately represent the mean path taken by a particle. However, because of their inertia, particles of all sizes do not respond in the same manner to turbulent fluctuations in the gas phase. Thus, it should be possible to neglect the effect of turbulent dispersion for some particles (thereby greatly simplifying the calculation of particle trajectories) without any loss of accuracy. This aspect of particle behaviour is studied here by comparing the trajectories with and without taking into account the turbulent dispersion effects.

In the present study, the above method is used to calculate the gas flow field and the trajectories of particles of given size, spatial distribution and velocity at the inlet in a range of flow conditions. The effect of turbulence on the particle motion was investigated by calculating the particle trajectories with and without turbulent dispersion effect. The results of these calculations are described below.

3 RESULTS AND DISCUSSION

The results of the calculations are discussed in three parts. In Section 3.1, the nature and development of the velocity field in a bend of circular cross-section is described. Special emphasis is placed here on the structure and development of secondary flow in the bend. In Section 3.2, typical particle trajectories are shown, and the role played by secondary flow and gas phase turbulence on the particle motion are discussed. Section 3.3 addresses a question of practical significance: given particle characteristics at the inlet, what percentage of them come out of the bend without depositing?

3.1 Nature of Axial and Secondary Flow in a Bend

With reference to the coordinate system depicted in Figure 1, the development of the axial velocity field in a 180-deg bend is illustrated in Figure 2a at bend angles, β, of 30, 60, 90 and 180 degrees from the inlet. These results were obtained for a Reynolds number of 236000 in a 180 deg bend of a bend-to-tube radius ratio of 24. Each cross-section is divided into two parts, the right half showing the experimental results of Rowe [3], and the left side showing the results obtained in the present study. It can be seen that the effect of the bend is already quite evident in the velocity contours at a β of 30 deg. The contours have now become non-concentric and the point of maximum velocity shifts towards the outer side of the bend. This process continues further, and by 60 deg, a significant radial gradient develops in the core region along the inner-outer diametrical plane. The distortion of the velocity field continues right up to the bend exit, although this is confined mainly to the inner side of the bend. Another point to note is that there is good agreement between the present predictions and the measurements of velocity field.

The development of the secondary flow field corresponding to this case is illustrated in Figure 2b. Here, the circumferential velocity, non-dimensionalised by the mean axial flow velocity, is shown at various bend angles. It can be seen that significant secondary flow develops quite early in the bend (within the first 15 deg), and that the shape of the profile shows little change with bend angle. An important point to note is that the circumferential velocity is maximum very close to the wall, and is more than 10% of the mean flow velocity for this flow condition. Thus, as far as particle motion is concerned, the circumferential flow is likely to have a strong effect when the particle is close to the wall.

A vector plot of the secondary flow in a 90-deg bend for the same conditions as above is shown in Figure 3. As expected, a relatively weak, double-vortex secondary flow is established very early in the bend, and continues to grow stronger as the bend angle increases. Such flow directs from the inner

side to the outer side of the bend in major part of the core, and reverses direction close to the wall.

3.2 Particle Trajectories

Particle motion in such three-dimensional flows as in curved ducts will be affected not only by the centrifugal force on the particle but also by the strong secondary flow present in the gas phase. The turbulence in the gas phase may also contribute to the dispersion of the particles. These and other aspects of particle motion in curved ducts are illustrated here qualitatively with reference to specific examples.

Figure 4 shows typical trajectories of particles in a 90 deg bend calculated using the FLOW3D code. In this case, the radius ratio R_c/R_t was 28 and the gas phase Reynolds number 1.07×10^6. A total of eight trajectories are shown in the figure. The four on the left half of the picture correspond to a particle size of 30 microns, while those in the right half are for a particle size of 300 microns. In each case, the continuous line represents the trajectory obtained without considering the turbulence dispersion effect. The other three trajectories, shown in broken lines, for each particle size include particle-turbulent eddy interaction. It should be noted that, because of the symmetry of the flow field about the inner-outer diametrical plane, all the eight particles have the same inlet location.

The role of the secondary flow and turbulent dispersion, and the effect of particle size on these factors, are clearly evident in the figure. The trajectory of the smaller particle is influenced strongly by both the secondary flow (curve 1) as well as by the turbulent dispersion (curves 2 to 4). The apparently random nature of the turbulent dispersion can also be seen in the entirely different paths followed by particles having exactly identical characteristics at the inlet, although even here there is evidence of the effect of the secondary flow in the gas phase.

In comparison, the motion of the larger particle is nearly insensitive to either the secondary flow (curve 5) or the turbulent dispersion effect (curves 6 to 8). It is entirely dominated by its inertia, and hardly deviates from its almost a straight path towards the outer wall. This behaviour of large particles is in accordance with the recent particle concentration measurements of Wang [2].

The effect (or its absence) of turbulent dispersion on the particle motion can also be seen in position and velocity of the particles at the point of their first impact with the wall. These are listed for the eight cases considered in Table 1. As in Figure 4, cases 1 and 5 correspond to particle motion without turbulent dispersion effect while in the other cases, this is included. It can be seen that in the case of the smaller particles both the point and velocity of impact show considerable scatter (with the fourth particle not hitting the wall at all) whereas all the larger particles deposit in a small patch. Also, they deposit very early into the bend (at a bend angle of 15 degrees) and have a much larger radial velocity than the smaller particles. This demonstrates that path of large particles is affected mainly by their inertia.

3.3 Overall Deposition Characteristics

As seen above, the particle trajectories in the bend are influenced mainly by their size, secondary flow in the gas phase and turbulent dispersion. The effect of these variables on the particle (droplet) flow through a bend can be illustrated in one parameter, namely, the percentage of particles deposited. This is shown in Figure 5 in which the overall percentage of particles (of uniform size and uniform spatial distribution at the inlet) deposited in a 180 deg bend is plotted as a function of the particle size with and without considering the effect of turbulent dispersion. These results were obtained for an air-droplet flow through a bend of R_c/R_t of 5 and an air flow Reynolds number of 68000. A total of 108 particles (water droplets) were used for each particle size. The graph shows that there appears to be a minimum particle size, in this case about 25 microns, above which all the particles deposit in the bend. As the particle size decreases below this threshold, more and more of them escape without deposition showing that their motion is strongly influenced by the secondary flow. For a particle size of 1 micron, almost all the particles come out of the bend indicating that these are completely entrained by the secondary flow, and are deflected away from the wall as they approach it.

The effect of turbulent dispersion on the percentage deposition is also summarized in Figure 5, in which results are presented with and without taking account of turbulent dispersion on the particles. For large particles, turbulent dispersion has little effect on the percent deposited. However, for smaller particles, the effect is significant in relative terms. For example, the percentage of deposition for 5 micron particles increases from 13% to 20%,

i.e., a relative increase of 50%, when turbulent dispersion effect is included. Another point to note is that inclusion of turbulent dispersion effect appears to increase the percentage deposited in all the cases considered. The reason for this is probably as follows. A particle which is entrained by the secondary flow spends quite a long time close to the wall. It will therefore deposit if, during this time, it acquires a sufficiently high radial velocity due to its interaction with a turbulent eddy.

The above conclusions are based on a relatively few number of calculations, and should therefore be treated as tentative and illustrative of the various effects rather definitive trends. More calculations, and over a wider range of Reynolds numbers, bend diameter ratios, particle characteristics and turbulent dispersion simulations should be carried out obtain a more complete picture of particle deposition in bends. One would then be in a position to develop an algebraic correlation for the percentage of particles deposited as they go through a bend. Calculations towards this end are in progress.

4 CONCLUSIONS

The simulation of the motion of particles through 90 and 180 deg bends of circular cross-section using CFD techniques shows that the curvature-induced secondary flow in the gas phase a strong effect on the particle trajectories in the bend. It appears that there is a threshold particle size below which particles may escape without depositing in a 180-deg bend. Turbulent dispersion of particles may play an important role in the motion of small particles.

ACKNOWLEDGEMENTS

The authors wish to acknowledge travel grants received from the German Academic Exchange Service (DAAD) and the British Council during the course of this work.

REFERENCES

(1) CROW, I., et al., The behaviour of certain feedwater solutes in a high pressure once-through boiler, *Proc. Inst. Mech. Engrs.*, 1979, bf 193, 349-354.

(2) WANG, M.J., Phasenverteilung, Sekundärströmung und Wärmeübergang bei Sprühkühlung in Krümmern. *Dr. Thesis*, Technical University of Munich, 1993.

(3) ROWE, M., Measurements and computations of flow in pipe bends. *J. Fluid Mech.*, 1970, **43**, 771-783.

(4) BAUGHN, J.W., et al., Local heat transfer measurements in turbulent flow around a 180-degree pipe bend. *J. Heat Transfer*, 1987, **109**, 43-48.

(5) JAYANTI, S., Contribution to the study of non-axisymmetric flows. *Ph.D. Thesis*, University of London, 1990.

(6) JONES, I.P., et al., FLOW3D, a Computer Code for the Prediction of Laminar and Turbulent Flow and Heat Transfer: Release 1. *UKAEA Report* No. AERE-R11825, 1985.

(7) RHIE, C.M. & CHOW, W.L., Numerical Study of the Turbulent Flow Past an Air Foil with Trailing Edge Separation. *AIAA J.*, 1983, **21**, 1527-1532.

(8) VAN DOORMAAL, J.P. & RAITHBY, G.D., Enhancement of the SIMPLE Method for Predicting Incompressible Flows. *Numer. Heat Transfer*, 1984, **7**, 147-163.

(9) RODI, W., Turbulence Models and Their Application in Hydraulics. *Experimental and Mathematical Fluid Dynamics*, 2nd ed.,1984.

(10) SCHILLER, L. & NAUMAN, A., Über die grundlegenden Berechnungen bei der Schwerkraftaufbereitung. *VDI*, 1933, **77**, 318-320.

(11) BURNS, A.D. & WILKES, N.S., A finite difference method for the computation of flows in complex three-dimensional geometries. *UKAEA Report* No. AERE-R12342, 1987.

(12) HUTCHINSON, P., HEWITT, G.F. & DUKLER, A.E., Deposition of liquid or solid dispersions from turbulent gas streams: A stochastic model. *Chem. Eng. Sci.*, 1971, **26**, 419-439.

(13) GOSMAN, A.D., & IOANNIDES, E., Aspects of computer simulation of liquid fueled combustors. *AIAA Paper No.* 81-0323, 1981.

Table 1 Deposition of particles in the 90-deg bend

No.	d_p [μm]	β_d [deg]	V_d/V_0 [-]
1	30	45.3	0.012
2	30	30.3	0.053
3	30	74.5	0.045
4	30	–	–
5	300	15.2	0.129
6	300	15.7	0.128
7	300	15.5	0.132
8	300	15.1	0.133

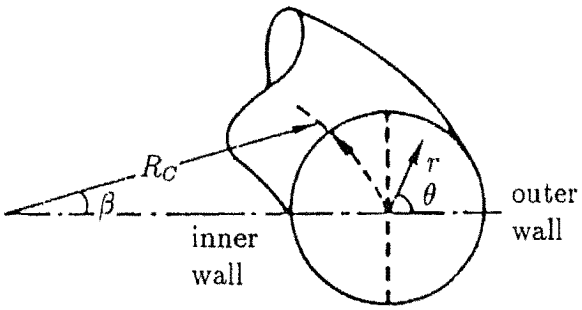

Figure 1 Coordinate system

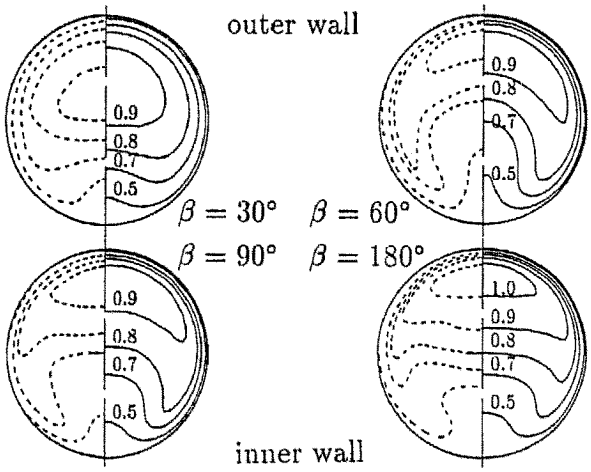

a) Contours of velocity head divided by $\varrho_g V_0^2/2$

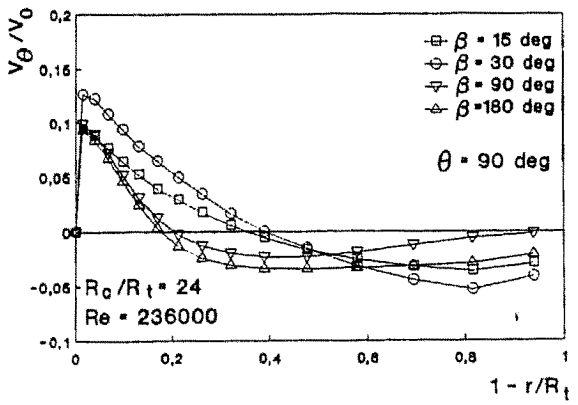

b) Secondary velocity profiles

Figure 2 Velocity fields in a 180 deg bend with $R_c/R_t = 24$ and $Re = 2.36 \times 10^5$

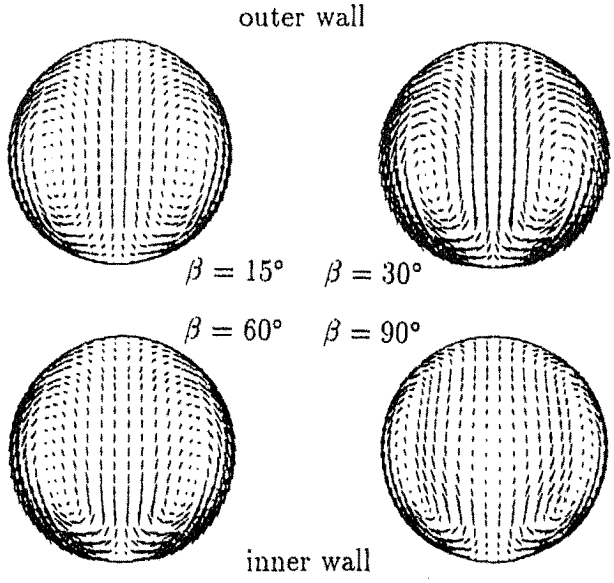

Figure 3 Secondary flow in a 90 deg bend with $R_c/R_t = 28$ and $Re = 1.07 \times 10^6$

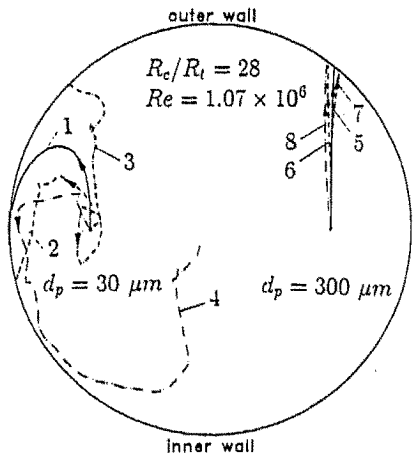

Figure 4 Particle trajectories in a 90 deg bend

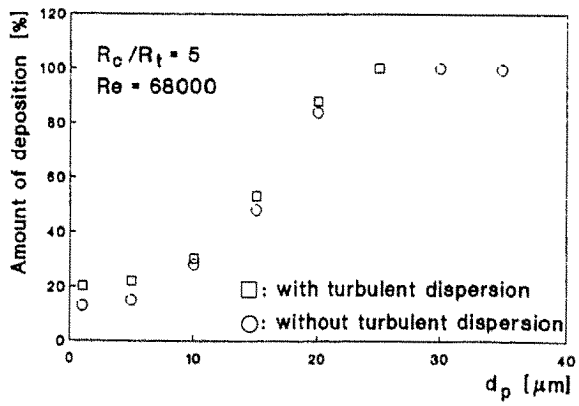

Figure 5 Behaviour of particle deposition in a 180 deg bend